



<b>Title</b>	Modelling of failure of structural textile composites
<b>Authors(s)</b>	Svensson, N., Gilchrist, M. D.
<b>Publication date</b>	2000-09-21
<b>Publication information</b>	Svensson, N., and M. D. Gilchrist. "Modelling of Failure of Structural Textile Composites." Springer-Verlag, September 21, 2000. <a href="https://doi.org/10.1007/s004660000176">https://doi.org/10.1007/s004660000176</a> .
<b>Publisher</b>	Springer-Verlag
<b>Item record/more information</b>	<a href="http://hdl.handle.net/10197/4831">http://hdl.handle.net/10197/4831</a>
<b>Publisher's statement</b>	The final publication is available at <a href="http://www.springerlink.com">www.springerlink.com</a>
<b>Publisher's version (DOI)</b>	10.1007/s004660000176

Downloaded 2026-05-01 23:44:22

The UCD community has made this article openly available. Please share how this access benefits you. Your story matters! (@ucd\_oa)



© Some rights reserved. For more information

# Modelling of Failure of Structural Textile Composite

N. Svensson and M.D. Gilchrist

*N. Svensson, Pelmatic Consulting Engineers, F O Petersons gata 28, SE-42131 VASTRA FROLUNDA, SWEDEN*

*M.D. Gilchrist, Department of Mechanical Engineering, University College Dublin, Belfield, Dublin 4, IRELAND*

Keywords: Textile composite, damage modelling, commingled yarns

## ABSTRACT

This paper summarizes extensive experimental work regarding the manufacture, mechanical characterization and modelling of textile thermoplastic composites produced by means of commingled yarns. These composites are believed to have a high potential for applications in structural automotive components. However, methods need to be developed for faster manufacturing and reliable prediction of the component mechanical performance and failure. A practical approach of finite element modelling of the stiffness and strength behaviour of these composites is briefly discussed.

## 1. Introduction

The continued successful usage of composite materials requires not only good mechanical performance but also fast manufacturing procedures. Glass Mat Thermoplastic (GMT) materials have proven their worth in large volume components in the automotive industry but their random fiber distribution and relatively low fiber volume fraction have limited the use to semi-structural applications. However, with the vast technology available in the textile industry there is much potential to accelerate the production process and to expand the range of mechanical properties and thus to develop new structural applications for composite materials.

The use of advanced textile preforms puts new demands on the models and procedures that are used for predicting component performance such as, for example, finite element analysis (FEA). New, and more accurate, material models, failure criteria and analysis procedures are required for an optimal design of composites components. This is

particularly true for those components fabricated using textile processes due to their complicated micro-structure.

The objective of the present work was two fold. Firstly, to study various aspects on manufacturing and the mechanical properties of novel textile commingled thermoplastic composites (glass fibers in a polyethylene terephthalate (PET) matrix). Secondly, by means of finite element modelling investigate the validity of an existing failure criterion and a progressive composite damage model. The mechanical properties for the laminates were determined in tension, in-plane shear, flexure, impact and interlaminar fracture. The results from the mechanical characterization were used for finite element analyses of the three-point bend test and also of an automotive structural component, i.e. a tow hook for a personal car. The mechanical performance of the composites and the correlation between the FE-analyses and the test results are discussed in the sections below.

## **2. Laminate Manufacture**

The laminates were produced by compression molding stacks of either a unidirectional warp knitted or a woven fabric with 5/6 of the fibers being oriented in the warp direction. The fabrics, shown in Fig. 1, were produced from air-jet texturized commingled yarns consisting of E-glass fibers (GF) and polyethylene terephthalate (PET) fibers, 50% by volume. The manufacturing and mechanical properties of commingled yarn composites have been extensively reviewed by the authors [1, 2].

Both the weaving and knitting processes used allowed for a fast manufacture with large freedom when tailoring the fabric. The amount of fibers in the warp and weft directions was easily changed and in the knitting process fibers with intermediate angles or layers of non-woven fibers could be included in the structure.

A textile characterization technique, the Kawabata Evaluation System, was successfully employed to estimate the formability and compressibility of the two fabrics and a reference wool fabric (a typical suit material). The degree of formability largely determines the possible geometric uses of a certain fabric while the degree of compressibility affects the required consolidation pressure during manufacture and hence influences the tooling and equipment costs. For these two specific configurations, the warp knitted fabric had a marginally higher formability than the woven fabric. Both the commingled yarn fabrics were more formable than the reference wool material, mainly due to the low shear losses and the high bending stiffness of glass fiber. More information on the measure of formability and the fabric properties involved are found in [2,3].

## **3. Mechanical Properties**

The static mechanical properties were determined in tension, flexure and in-plane shear [2] and are detailed in Table I and figure 2. Under conditions of flexure the warp knitted laminates were stronger and stiffer than the woven laminates in the warp direction while the woven laminates were stronger and stiffer when tested in the weft direction. This was due to the fraction of reinforcing glass fibers in the weft yarns of the woven laminates. The values of the moduli were significantly higher in flexure than in tension and these are in good agreement with the values predicted by the rule of mixtures equation. The laminate quality was examined using optical microscopy (OM) and scanning electron microscopy

(SEM). Few voids were present and the consolidation quality was generally good. However, adhesion between the glass fibers and the thermoplastic matrix was poor.

Low velocity impact characterization was carried out by means of a drop weight test. The impactor was a hemisphere with a radius of 5 mm. The weight of the impactor was 14.3 kg and the drop height 1m resulted in an impact energy of about 140 J and an impact velocity of 4.4 m/s. Extensive delaminations and cracking occurred in both materials. Plastic deformation of the matrix and a considerable amount of fiber fracture took place during the impact. If the area of delamination is considered as a measure of impact resistance, the woven laminates proved superior to the warp knitted laminates, which in some cases almost completely split up along the mid-plane. The flexural failures were gradual, which indicated the ability of the material to absorb large amounts of energy. The fiber architecture of the woven laminates tended to limit the extent of delamination efficiently due to the interlacement of the warp and weft yarns. The slight fiber misalignment in the fabrics, the formation of resin pockets during manufacturing and the poor fiber/matrix interface, which led to extensive fiber pull-out all contribute to a high apparent fracture toughness of the two materials.

The fracture toughness values in pure Mode I, pure Mode II and mixed modes (loading ratios I:II = 4:1, 1:1 and 1:4) were determined by means of the Double Cantilever Beam test (DCB) and the Mixed Mode Bending test (MMB) [4]. The fiber architectures that had been used contributed to the high interlaminar toughness values that were observed by introducing numerous failure mechanisms, such as cusp formation, matrix shearing, matrix cracking, fiber pull-out, resin pockets and fiber bridging. The fracture toughness is shown in Table II. Figure 3 shows a fracture surface from a woven mixed mode I:II=1:1 interlaminar fracture. A resin pocket, fiber pull-out and fiber breakage are seen. The very clean fibers are evidence of the poor fiber/matrix adhesion. Compared to traditional thermoset matrix composites the crack initiation and propagation toughness is higher for these materials. Models for predicting mixed mode delamination in prepreg and textile composites have been developed by the author and are discussed in detail elsewhere [5,6].

Very little is known about the fatigue performance of thermoplastic textile composites. For this reason, the woven laminates were also subjected to flexural fatigue loading [5]. A decrease in failure load to about 60% of the maximum static flexural strength was observed after  $10^6$  load cycles. The scatter in the fatigue results was comparable to that normally observed during composites fatigue testing. The fatigue failures were initiated by damage at the micro-structural level which, as the number of load cycles continued, developed into a damage zone that grew until ultimate failure occurred. The damage mechanisms were similar to those observed in static flexural tests and impact tests, which indicated that the material behaviour was consistent and reasonably independent of the loading conditions and loading rates.

#### **4. FE-modelling**

A practical approach to modelling the material behaviour of these textile composites was evaluated. The aim of this was to enable the use of composite mechanical data obtained from simple standard tests in a manner that provided a satisfactory prediction of structural stiffness and strength.

The three-point bend test was chosen for the FE-modelling as it enabled simple verification with the experimentally determined results. The test set-up and specimen dimensions were as follows; support span = 48 mm, width = 23 mm and thickness = 3.25 mm. The cylindrical steel load head had a diameter of 6 mm. The loading head and supports were assumed to be rigid when compared to the specimen. A displacement of 2.5 mm was applied to the loading head in the z-direction. The composite specimen was represented by 288 8-noded shell elements with an element length of 2 mm. The analyses were carried out using ABAQUS Standard v5.6 with I-DEAS Master Series 4.0 as the pre- and post-processor.

The laminate was modeled by layered shell elements with twelve layers of an orthotropic material. Unidirectional  $(0^\circ)_{12}$  and symmetric cross-ply  $(90^\circ/0^\circ/90^\circ/0^\circ/90^\circ/0^\circ)_s$  lay-ups were used. The use of Classical Laminate Theory for the representation of multi-layer textile thermoset and thermoplastic composites has previously been applied successfully for automotive structural components [7,8]. The mechanical property data determined in the tests described earlier were used for the lamina data in the lay-ups. A combined failure model and material softening model, developed by Chang and Chang [9, 10], which separately accounts for fiber buckling, tensile matrix cracking, compressive matrix failure, fiber/matrix shear failures and matrix shear softening due to damage accumulation was implemented in ABAQUS [11] by a user subroutine and applied to the laminae. In the model the lamina properties are updated after all failure events. For example, after the occurrence of matrix failure the lamina transverse modulus and the Poisson's ratio are set equal to zero.

Using the Tsai-Hill criterion to determine first ply failure, very good agreement with the experimental data was obtained for the unidirectional as well as for the cross-ply laminates. The predicted deflections at initial failure were 2.40 mm and 1.93 mm respectively and the observed deflections were 2.35 mm for the unidirectional laminates and 1.96 mm for the cross-ply laminates. The failure model gave a reasonable agreement with the experimentally determined load/deflection trace, figure 4. This failure model was originally developed and verified for notched carbon fiber prepreg laminates loaded in-plane where it was seen to provide a good agreement with the observed failures [7,8]. However, the assumptions made by Chang and Chang regarding the failure mechanisms could not be directly transferred to the more complex thermoplastic textile composites. Also, no data was available for the shear softening of the matrix as a function of strain and a value similar to that used by Chang and Chang was used. The matrix cracking predicted by the analysis, figure 5, agreed well qualitatively with the cracking that was observed on the three point bending specimens. The SEM micrograph in figure 6 shows the appearance of the surface of the specimen where matrix cracking has taken place.

For a further validation of the computational models a tow hook for a personal car was modeled and analyzed. The simulation resembles the event of a car reversing into a concrete bollard, figure 7. The composite tow hook consists of a polyurethane foam core with a glass fiber/PET skin. The fiber angles used were  $0^\circ/+55^\circ/-55^\circ$  to obtain stiffness axially as well as in torsion. The proposed manufacturing of the hook involves the winding of axial fabrics around the core, which is then over-braided and finally the hook is consolidated by the application of heat and pressure. The reason for studying a composite

tow hook is of course to reduce the mass of the complete vehicle and hence to improve performance by reducing fuel consumption and environmental damage. Early results also indicate that the composite tow hook would come out favorably in a life cycle analysis (LCA) when compared to a traditional steel hook.

The foam core was modeled using solid 4-noded elements while the laminates were represented by 3-noded thin shell elements. The ABAQUS material model for crushable foam including effects of foam hardening was used for the core. Material data for typical polyurethane foam was taken from an example in the ABAQUS/Explicit Example Problems Manual. The damage model described previously in this section was applied to the lamina material. The element size in the entire model was kept as uniform as possible to facilitate use in explicit analyses. The concrete bollard was considered rigid when compared to the composite skins and the surface of the bollard was modeled using rigid shell elements. Due to symmetry only half of the hook was analyzed and symmetric boundary conditions were applied to the nodes at the mid-surface cross section. The low mass of the hook when compared to the mass of the entire car justified the assumption of clamped boundary conditions at the hook connection to the rear car body. The motion was simulated by forcing a displacement of the bollard into the hook. Contact was defined between the laminate skin and the bollard with coefficient of friction that was estimated to be 0.5.

Figure 7 shows the calculated Von Mises stresses in the foam core. As expected, the highest stresses occurred locally within the bollard where the foam is compressed and at the compression side of the base of the hook [12]. In figure 8 the predicted extent of damage in the composite skin of the hook impacted by the bollard is shown.

The manufacture, analysis and testing of the tow hook constitutes work that is still in progress. Attempts have been made to produce thermoplastic hooks using internal pressure bladder molding [8]. Also, thermoset matrix hooks have been produced by means of resin transfer molding (RTM) and here carbon fiber as well as glass fiber textile preforms were used as reinforcement. The aluminum tool was initially designed to accommodate both the thermoplastic and the thermoset manufacturing routes. A number of the physical hooks that have been produced are currently undergoing a variety of tests to validate the performance. Tests regarding stiffness and fatigue are carried out according to automotive industry standards and when these are finished the natural subsequent step is to validate the FE-predictions regarding stiffness and damage evolution and progression [13-15].

Throughout the project a number of areas where future research is necessary have been identified. These concern manufacturing, mechanical properties as well as modelling of commingled and textile composites. Some specific proposals are listed below:

- A sensitivity analysis of the material mechanical properties used in the progressive failure model should be carried out to determine the accuracy required in the acquisition of mechanical laminae data.
- An adaptation of the failure model for use in ABAQUS/Explicit would facilitate numerical analyses of contact and dynamic events, such as collisions, of composite components.

- The further development of modelling processing parameters (as reviewed in [1]) is essential to provide tools for the accurate prediction and optimization of the component production, reducing the relatively large amount of trial and error currently involved in composite manufacture.
- The detailed modelling of the failure mechanisms occurring in textile composites leading to useful failure criterion. However, this is a paramount task and it is doubtful that a single model will ever be able to represent all of the variations available in today's textile composites.
- A study of the effects of notches on the mechanical performance in thermoplastic textile composites but also GMT type materials. Design recommendations for static notched strength as well as fatigue durability are scarce in literature.

## 5. Conclusions

The mechanical performance of textile thermoplastic matrix composites was determined. Compression molding of woven and warp knitted commingled yarn fabrics produced high quality laminates with good mechanical properties. The complex fiber architecture contributed to the high fracture toughness and impact resistance observed, as did the poor adhesion between the glass fibers and the PET matrix. The laminate fatigue performance was seen to be equal to comparable composites. It can be concluded that these composite materials offer significant scope for use in the production of large volume composite structural components, i.e. areas where SMC and GMT material do not offer sufficient stiffness, strength or durability.

In a series of FE-analyses, the Tsai-Hill failure criterion predicted initial failure of the laminates well, at least for the simple lay-ups and stress states analyzed here. The damage model proposed by Chang and Chang provided only adequate agreement with the experimental results. A more thorough analysis and adaptation of the parameters in the model will have to be made to enable application also for the more complex fiber architectures in textile composites. Future work will evaluate this material in larger and more complex components, such as the tow hook described briefly.

### *Acknowledgements*

The authors are grateful to the Swedish Institute for Fibre and Polymer Research, with whom aspects of this research have been carried out.

### *References*

1. Svensson, N., Shishoo, R. and Gilchrist, M., 1998, 'Manufacturing of thermoplastic composites from commingled yarns - A review', Journal of Thermoplastic Composite Materials, Vol. 11, pp. 22-56.
2. Svensson, N., Shishoo, R. and Gilchrist, M., 1998, 'Fabrication and mechanical response of commingled GF/PET composites', Polymer Composites, Vol. 19, No. 4, pp. 360-369.

3. Shishoo, R., and Choroszy, M., 1990, 'Fabric Tailorability', *Textile Asia*, December 1990, pp. 64-69.

4. Svensson, N., Gilchrist, M. and Shishoo, R., 1998, 'Interlaminar fracture of commingled GF/PET composite laminates', *Journal of Composite Materials*, Vol. 32, No. 20, pp. 1808-1835.

5. Gilchrist, M., Svensson, N. and Shishoo, R., 1998, 'Fracture and fatigue performance of textile commingled yarn composites', *Journal of Materials Science*, Vol. 33, pp. 4049-4058.

6. Svensson, N. and Gilchrist, M., 1998, 'Mixed-Mode Delamination of Multidirectional Carbon Fibre/Epoxy Laminates', *Mechanics of Composite Materials and Structures*, Vol. 5, pp. 291-307.

7. Svensson, N., Shishoo, R. and Gilchrist, M., 1999, 'Tensile and flexural properties of textile composites', *Journal of the Textile Institute*, Vol. 89, No. 1(4), pp. 635-646.

8. Svensson, N., Tollemark, P. and Hansson, W., 1997, 'Hollow structural thermoplastic composites', in proceedings of Tectextil Symposium, 12-14 May, Frankfurt am Main, Germany.

9. Chang, F.-K. and Chang, K.-Y., 1987, 'Post-failure analysis of bolted composite joints in tension or shear-out mode failure', *Journal of Composite Materials*, Vol. 21, pp. 809-833.

10. Chang, F.-K. and Chang, K.-Y., 1987, 'A progressive damage model for laminated composites containing stress concentrations', *Journal of Composite Materials*, Vol. 21, pp. 834-855.

11. ABAQUS/Standard User's Manual, Examples, Version 5.6, Hibbitt, Karlsson & Sorensen, Inc, USA.

12. Naganarayana, B. P. & Atluri, S. N., 1995, 'Strength reduction and delamination growth in thin and thick composite plates under compressive loading,' *Computational Mechanics*, Vol. 16, pp. 170-189.

13. Kim, K. D., Park, T. & Voyiadjis, G. Z., 1998, 'Postbuckling analysis of composite panels with imperfection damage,' *Computational Mechanics*, Vol. 22, pp. 375-387.

14. Krawczuk, M., Ostachowicz, W. & Zak, A., 1997, 'Dynamics of cracked composite material structures,' *Computational Mechanics*, Vol. 20, pp. 79-83.

15. Ousset, Y. & Roudolff, F., 1997, 'Numerical analysis of delamination in multilayered composite plates,' *Computational Mechanics*, Vol. 20, pp. 122-126.

## Captions

Figure 1. Optical micrographs detailing the warp-knitted (left) and woven (right) unidirectional fabrics.

Figure 2. The SEM micrograph is showing a tensile failure in a woven laminate. Extensive delaminations, fiber pull-out and fiber bridging have occurred.

Figure 3. A fractured resin pocket on the surface of a woven mixed mode I:II=1:1 interlaminar fracture. Fiber pull-out and fiber fracture can be seen in the micrograph. The very clean fibers indicate poor adhesion between the matrix and the glass fibers.

Figure 4. The correspondence between the experimentally determined load/deflection trace and the predicted trace of the damage model.

Figure 5. The predicted progression of matrix cracking at the end of the three-point bend test.

Figure 6. The micrograph shows the surface of the specimen in the area where matrix cracking did occur.

Figure 7. The FE-model of the tow hook and the XXX. The plot contours the calculated stresses in the polyurethane foam core at the end of the event.

Figure 8. The plot shows the predicted amount of failure in the composite skin.

Table I. The experimentally determine mechanical properties of the unidirectional woven and warp-knitted laminates.

Table II. The mode I, mode II and mixed modes 4:1, 1:1 and 1:4 interlaminar fracture toughness values for the warp knitted and the woven laminates.

## Tables

Property	Woven	Warp knitted
Tensile modulus, 0°/90°, (GPa)	22.9/6.9	28.2/3.5
Tensile strength, 0°/90°, (MPa)	510/131	487/7
In-plane shear modulus, (GPa)	4.4	4.3
In-plane shear strength, (MPa)	98.7	88.4
Flexural modulus, 0°/90°, (GPa)	29.0/10.7	35.0/4.6
Flexural strength, 0°/90°, (MPa)	494/214	747/25

Table I. The experimentally determine mechanical properties of the unidirectional woven and warp-knitted laminates.

	Woven	Warp knitted
$G_{IC}$ initiation, (kJ/m <sup>2</sup> )	1.13	0.89
$G_{IC}$ propagation, (kJ/m <sup>2</sup> )	1.34	1.14
$G_{IIC}$ initiation, (kJ/m <sup>2</sup> )	1.32	0.97
$G_{IIC}$ propagation, (kJ/m <sup>2</sup> )	2.80	2.55
$G_{4:1C}$ initiation, (kJ/m <sup>2</sup> )	1.01	1.28
$G_{4:1C}$ propagation, (kJ/m <sup>2</sup> )	1.42	1.79
$G_{1:1C}$ initiation, (kJ/m <sup>2</sup> )	1.20	1.04
$G_{1:1C}$ propagation, (kJ/m <sup>2</sup> )	1.96	1.69
$G_{1:4C}$ initiation, (kJ/m <sup>2</sup> )	1.11	1.39
$G_{1:4C}$ propagation, (kJ/m <sup>2</sup> )	2.23	2.62

Table II. The mode I, mode II and mixed modes 4:1, 1:1 and 1:4 interlaminar fracture toughness values for the warp knitted and the woven laminates.

## Figures

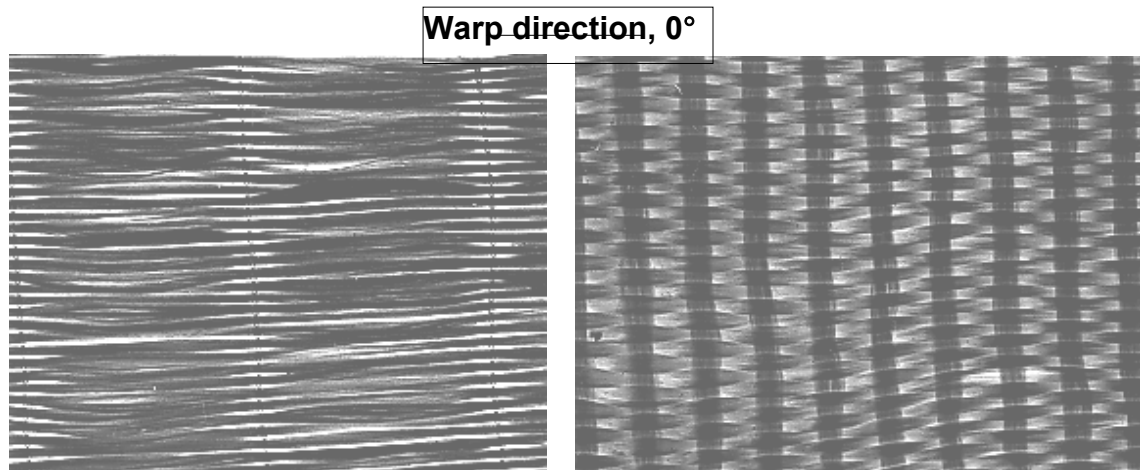


Figure 1. Optical micrographs detailing the warp-knitted (left) and woven (right) unidirectional fabrics.



Figure 2. The SEM micrograph is showing a tensile failure in a woven laminate. Extensive delaminations, fiber pull-out and fiber bridging have occurred.

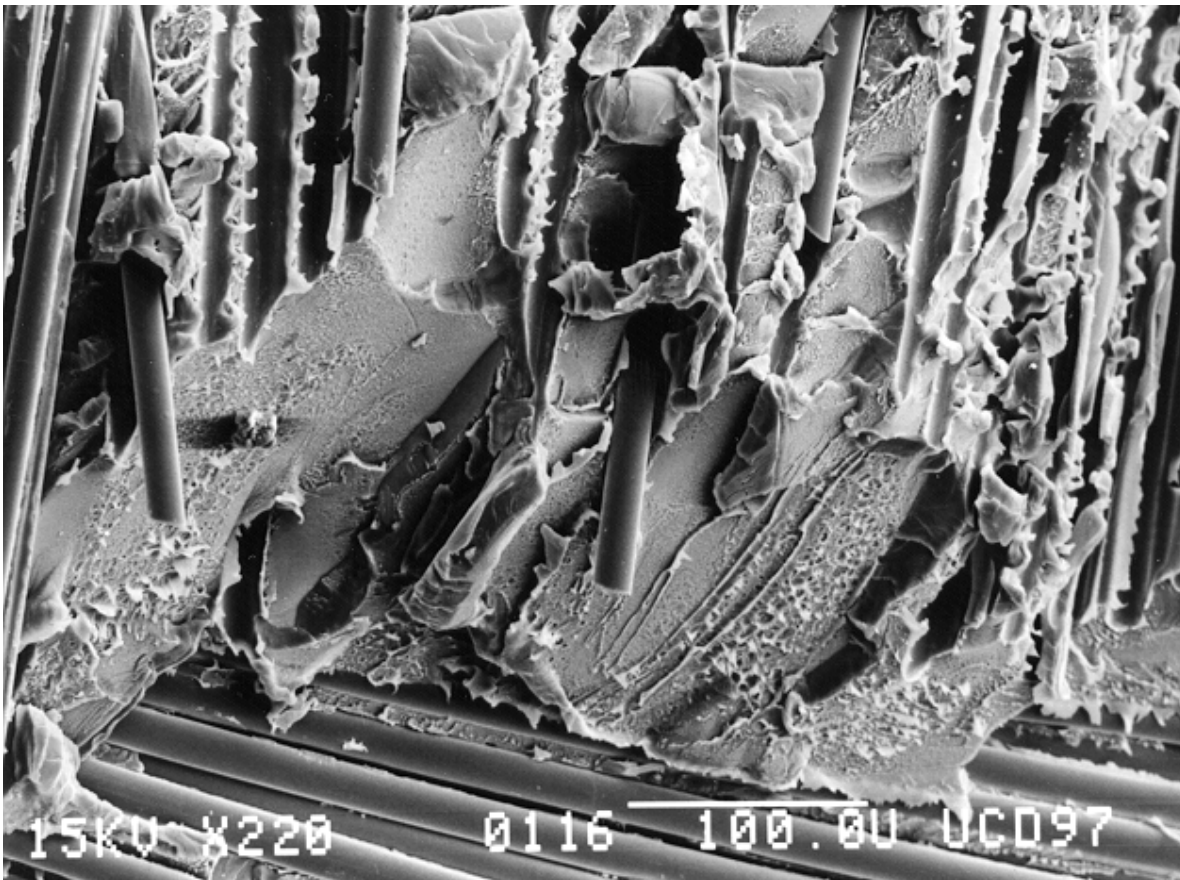


Figure 3. A fractured resin pocket on the surface of a woven mixed mode I:II=1:1 interlaminar fracture. Fiber pull-out and fiber fracture can be seen in the micrograph. The very clean fibers indicate poor adhesion between the matrix and the glass fibers.

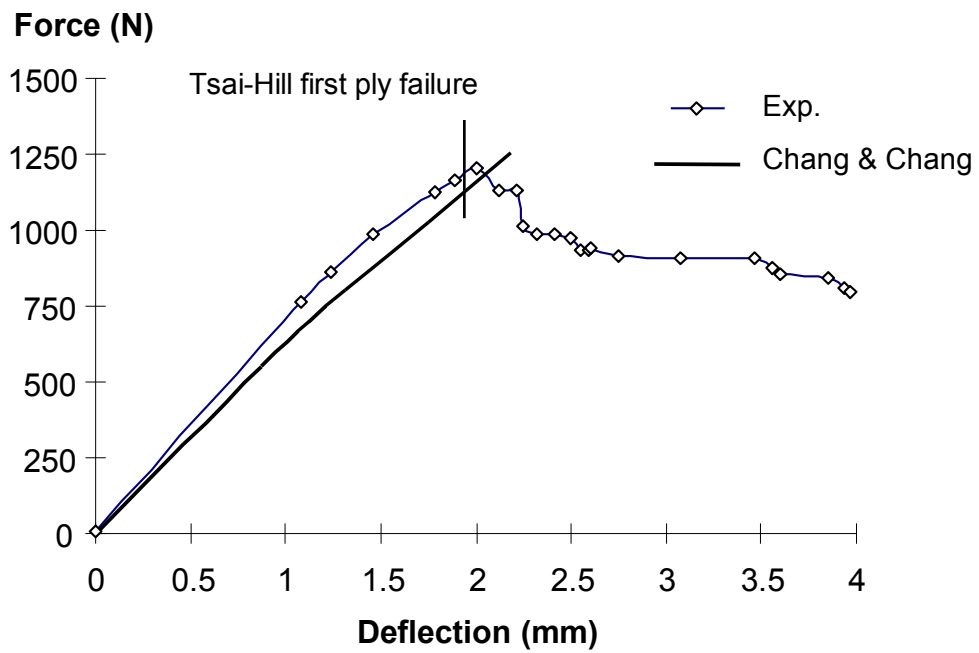


Figure 4. The correspondence between the experimentally determined load/deflection trace and the predicted trace of the damage model.

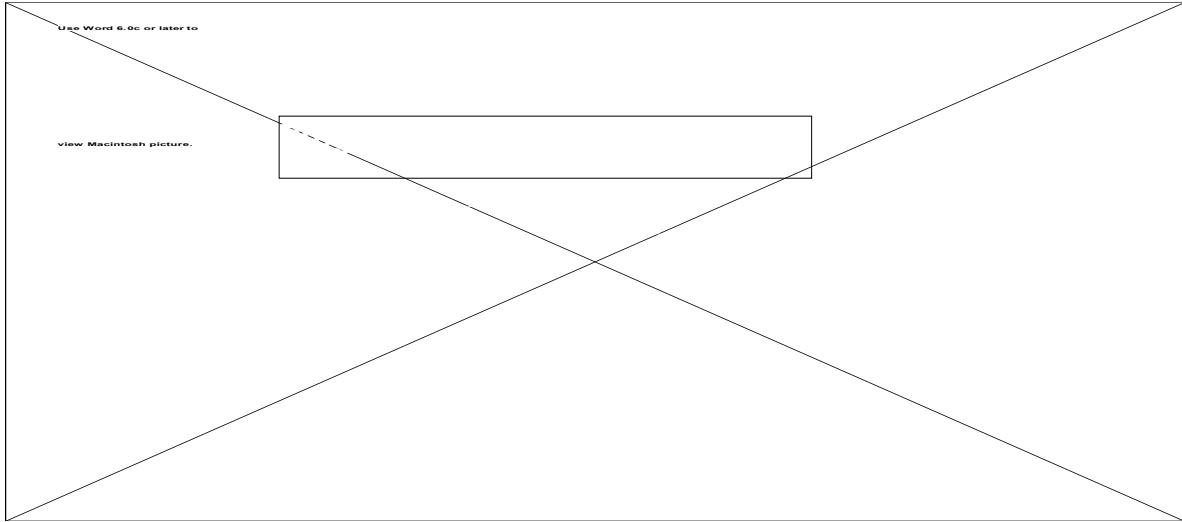


Figure 5. The predicted progression of matrix cracking at the end of the three-point bend test.

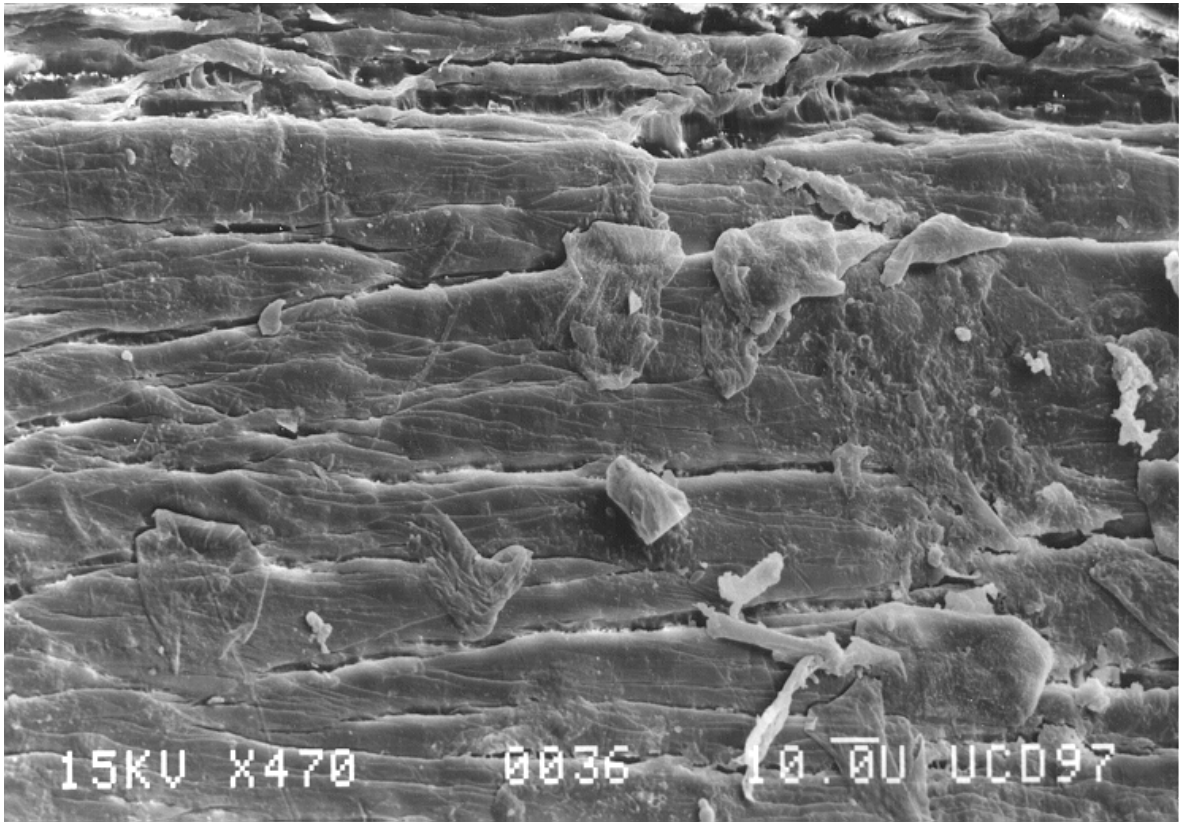


Figure 6. The micrograph shows the surface of the specimen in the area where matrix cracking did occur.

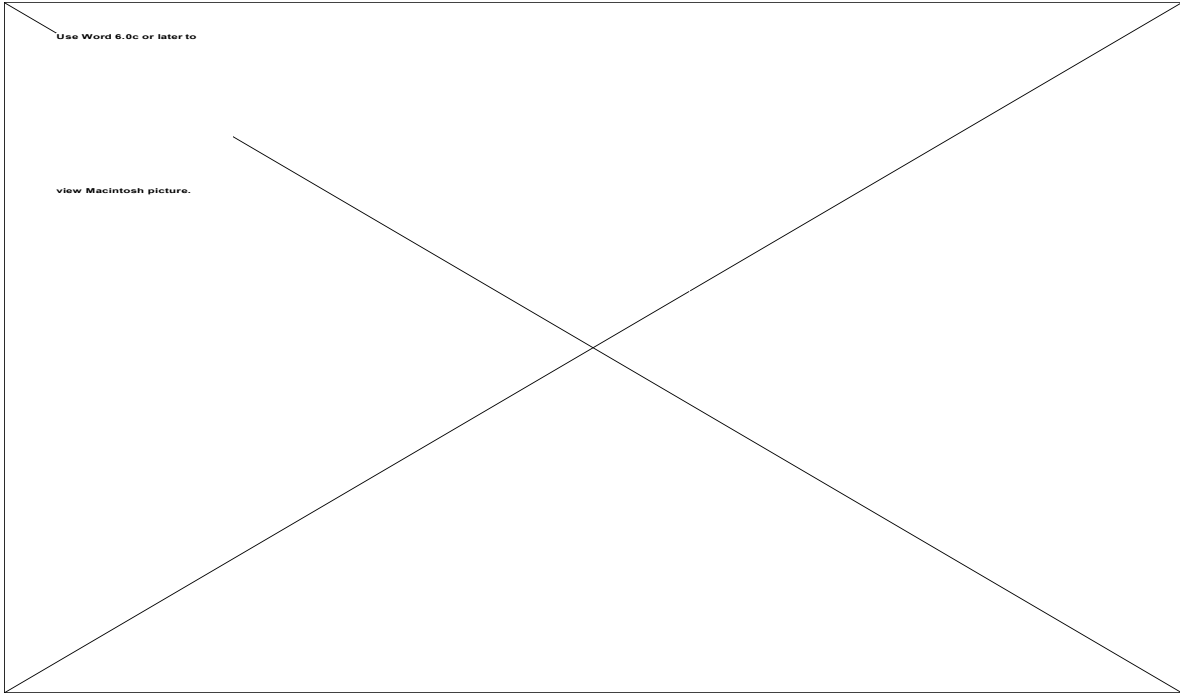


Figure 7. The FE-model of the tow hook and the bollard. The plot contours the calculated Von Mises stresses in the polyurethane foam core at the end of the impact event.

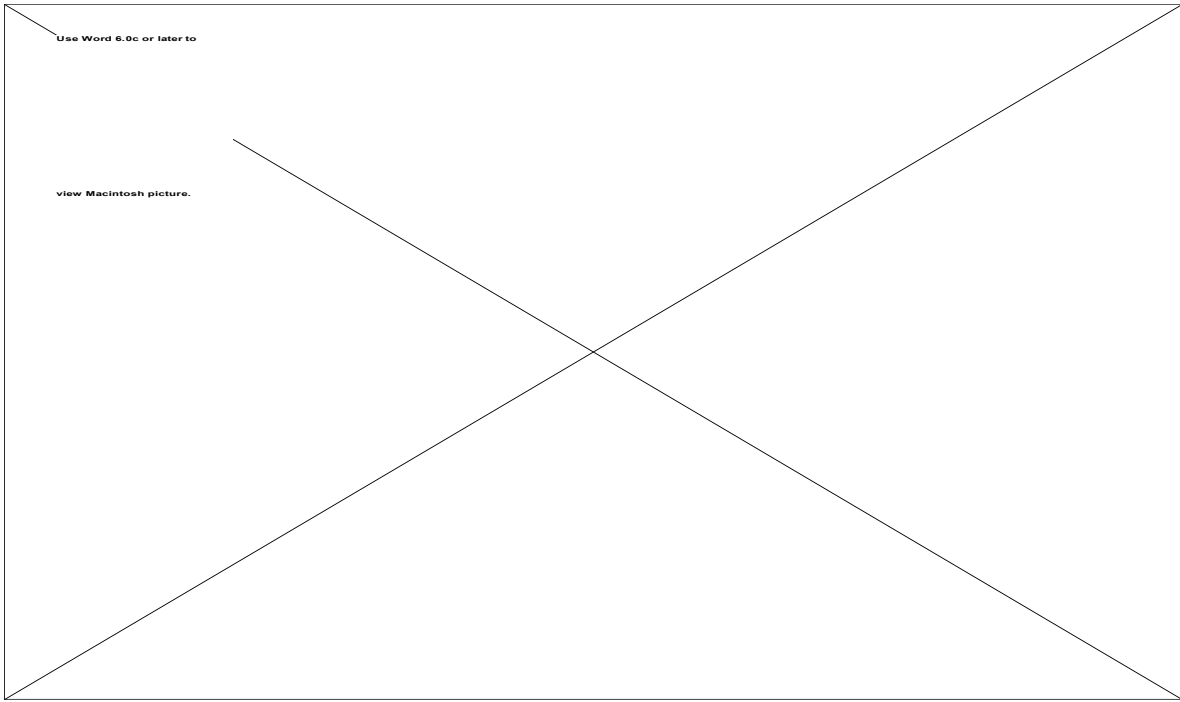


Figure 8. The plot shows the predicted amount of failure in the composite skin.